

Analyzing Impacts of FACTS Devices in Dealing with Short-Term and Long-Term Wind Turbine Faults

A. Shahdadi¹, B. Z-M-Shahrekohne², S. M. Barakati^{1,*}

¹Department of Electrical and Computer, University of Sistan and Baluchestan, Iran.

²Department of Electrical, Computer and Biomedical Engineering, University of Pavia, Italy.

Abstract- More than one hundred countries are using wind energy due to their easy implementation, cheap energy, and high energy efficiency. Implementation of FACTS devices in Wind Energy Conversion Systems (WECS) has been dramatically improved due to cooperative and accurate performance of FACTS devices. However, dealing with wind turbine faults promptly is crucial. Short-term and long-term faults may have excessive voltage changes and inconstant active and reactive power injection into transmission line. In this paper, robustness and flexibility of SSSC, STATCOM, and UPFC FACTS devices connecting to a 9 MW SCIG-based wind farm under different time-domain fault conditions is investigated. Variety of system scenarios under fault conditions are surveyed in order to find the best Fault Ride Through (FRT) scheme for the system. To carry out this study, same rating and capacity is considered for all three FACTS devices which are employed at the grid-connected point of WECS to mitigate FRT problem. Moreover, the best compromised control mode of FACTS devices is sought by a power flow analysis. Additionally, to obtain a more perceivable view over the technical issues related to the voltage sag support, performance of FACTS devices is analyzed and compared with each other through the paper and at the final stage. A complete digital simulation of the system is executed in the MATLAB/SIMULINK environment and the results are presented to authenticate the performance of devices.

Keyword: Wind Energy Conversion System; Flexible AC Transmission System; Fault Ride Through; Squirrel Cage Induction Generator; Static Synchronous Series Compensator; Static Synchronous Compensator ; Unified Power Flow Controller

1. INTRODUCTION

Wind energy implementation is growing very fast around the world. As of today, wind power sustains 10.4% of the total electricity demand of EU's electricity. To this reason, necessity of developing wind energy technology and solving barriers relating to them is of great importance. Wind power is one of the lowest-priced, costing between four and six cents per kilowatt-hour. However, to guarantee this low price power generation and high-efficiency, appropriate maintenance of wind farms is vital [1].

When wind turbines are connected to the grid, they provide active power to the grid, but simultaneously, they absorb reactive power from the grid which this can lead to lack of reactive power for the grid if not compensated

Received: 16 Dec. 2018

Revised: 09 Feb. 2019

Accepted: 11 May 2019

*Corresponding author: (S. Masoud Barakati)

E-mail: smbaraka@ece.usb.ac.ir

Digital object identifier: 10.22098/joape.2019.5591.1420

Research Paper

© 2019 University of Mohaghegh Ardabili. All rights reserved.

in time [2]. Therefore, if the safe operation of the system besides the continuous integration of the wind farm is desired, reactive power should be maintained in order to avoid voltage fluctuations and system failure [4] [8]. By occurrence of a fault in the system, generator terminal voltage of the WECS begins to drop [27]. This situation causes electrical torque to follow a down trend and abruptly fall to zero and rotor speed to rise up [4-5]. Though, utilization of the FACTS devices can ensure the reactive power compensation of the system and therefore system stability. Implementation of FACTS devices however costly can guarantee wind turbine connection to the grid during fault conditions [7-8]. A variety of FACTS devices are suggested for improvement of power system performance in literatures [9-12]. Dixon, et al, has discussed implementation and reactive power compensation for variety of FACTS devices [13]. In [18], a frequency domain analysis in order to design a controller for static synchronous series compensator (SSSC) is used with the aim of system stability improvement; however, as a series-based FACTS device, SSSC has the main drawback of resonance phenomena [17]. Ghassemi, et al, proposed a STATCOM transient

stability model for dealing with small-disturbance stability issues, but this model is supposed to be used together with auxiliary damping controls, which could be a problem for power system designers and operators [10]. In [14], application of STATCOM in order to enhance voltage stability of the wind power is studied for short-term faults, but faults with long-term time-domain are not investigated. In [27], a nonlinear backstepping controller for LVRT capability enhancement in PMSG-based wind turbine is proposed. In [11], a UPFC is connected to a doubly-fed induction generator (DFIG)-based WECS to overcome voltage sags during faults for two special grid codes. Although application of UPFC prospered safety margin of the system to some extent, this improvement is achieved only in certain levels of voltage and not in entire levels. In [15], the impacts of using UPFC and STATCOM on protection system are compared; however, long-term faults of the system are not discussed again.

This paper’s main contribution is time-domain responses of SSSC, STATCOM, and UPFC for both short-term and long-term faults in an on-grid wind energy conversion system (WECS).

The next parts of this paper are arranged as follows: Section II, designates SSSC, STATCOM, and UPFC main structures concisely. Section III, put forward case under study in this paper. Section IV, concentrates on control theory behind FACTS. Section V, illustrates simulation results, and finally section VI, is devoted to conclusion.

2. COMPENSATION OF FACTS DEVICES

There is a considerable unemployed potential in transmission lines which inspires engineers to head for reconfiguration of power systems and using additional devices [16]. FACTS devices incorporating power electronic-based and other static controllers provide transmission grids controllability and ability to accommodate with changes, while maintaining sufficient steady-state and transient margins through operating conditions [17]. Installing additional devices such as FACTS at the terminals of the wind turbine or at the substation (in case of wind parks) to provide the required voltage support is necessary to fulfill the FRT requirements [25]. FACTS devices can be used as an alternative to reduce the flows in systems with heavily loaded lines. This usage will result in increment of system loadability, decrement of system losses, and improvement of system stability. Additionally, FACTS devices have promising application in WECS [9] [20] [26]. For instance, due to existence of a few inherent defects in IG-based WECS, such as high sensitivity to

grid faults, an appropriate designation of a FACTS controller can significantly improve system stability and avoid voltage drop at the IG terminals [11].

2.1. Static synchronous series compensator

As part of the flexible AC transmission system device family, SSSCs have been employed for power management of wind farms in many literatures by researchers [18-21]. SSSC can provide capacitive or inductive voltage independent of the line current up to its specified current rating. Moreover, SSSC is capable of negotiating both active and reactive power with the ac system, simply by controlling the angular position of the injected voltage. The capability of SSSC to exchange active power has significant application potentials, simultaneous compensation of the inductive and resistive components of the series line impedance, in order to keep the X/R ratio high, can be named as one. The SSSC contains a solid-state voltage source inverter connected in series with the transmission line through an insertion transformer. This connection enables SSSC to control power flow in the line for a wide range of system conditions [21].

The fundamental schematic of SSSC, shown in Fig. 1, can be derived based on operation principle of SSSC. In the equivalent, the SSSC is represented by a voltage source V_{se} in series with a transformer impedance. In the practical operation of the SSSC, V_{se} can be regulated to control the power flow of line i-j or the voltage at bus i or j.

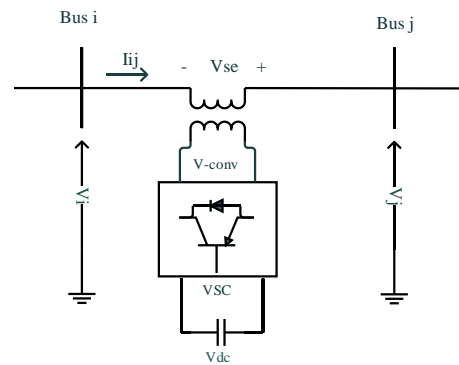


Fig. 1. Fundamental schematic circuit of SSSC

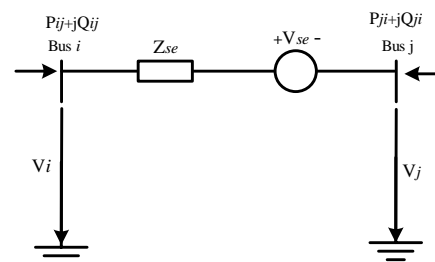


Fig. 2. Equivalent circuit of SSSC

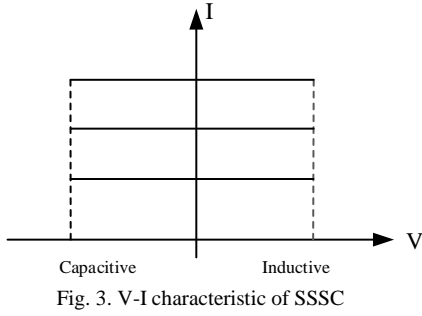


Fig. 3. V-I characteristic of SSSC

In the equivalent circuit, $V_{se}=V_{se} \angle \theta_{se}$, $V_i=V_i \angle \theta_i$, $V_j=V_j \angle \theta_j$, assuming SSSC operating in active power flow control mode, the exchanged power between buses i - j can be calculated as:

$$P_{ij} = V_i^2 g_{ii} V_i V_j \begin{pmatrix} g_{ij} \cos \theta_{ij} \\ +b_{ij} \sin \theta_{ij} \end{pmatrix} - V_i V_{se} \begin{pmatrix} g_{ij} \cos(\theta_i - \theta_{se}) \\ +b_{ij} \sin(\theta_i - \theta_{se}) \end{pmatrix} \quad (1)$$

$$Q_{ij} = -V_i^2 b_{ii} V_i V_j \begin{pmatrix} g_{ij} \sin \theta_{ij} \\ +b_{ij} \cos \theta_{ij} \end{pmatrix} - V_i V_{se} \begin{pmatrix} g_{ij} \sin(\theta_i - \theta_{se}) \\ +b_{ij} \cos(\theta_i - \theta_{se}) \end{pmatrix} \quad (2)$$

where $g_{ij}+jb_{ij}=1/Z_{se}$, and g_{ij} and b_{ij} are conductance and susceptance between buses i and j , respectively. The equivalent circuit and V - I characteristic of SSSC are presented in Fig 2 and Fig. 3, respectively.

2.2. Static Compensator (STATCOM)

STATCOM is another flexible AC transmission system device which is operating via solid state switching converter connected in parallel to the grid through a coupling transformer. The main structure of STATCOM is composed of a DC link capacitor and a voltage source converter (VSC) which makes it possible for the device to form a mutual interface with the power system [14]. Fig. 4 illustrates fundamental schematic of STATCOM. Power system requirements can be dealt with by controllable injection/absorption of real and reactive power in STATCOM output terminal at fundamental frequency due to power electronic equipment [22].

According to the equivalent circuit of the STATCOM shown in Fig. 5, suppose $V_{se}=V_{se} \angle \theta_{se}$, $V_i=V_i \angle \theta_i$, then the power flow constraints of the STATCOM are:

$$P_{sh} = V_i^2 g_{sh} - V_i V_{sh} \begin{pmatrix} g_{sh} \cos(\theta_i - \theta_{sh}) \\ +b_{sh} \sin(\theta_i - \theta_{sh}) \end{pmatrix} \quad (3)$$

$$Q_{sh} = -V_i^2 b_{sh} - V_i V_{sh} \begin{pmatrix} g_{sh} \sin(\theta_i - \theta_{sh}) \\ -b_{sh} \cos(\theta_i - \theta_{sh}) \end{pmatrix} \quad (4)$$

where $g_{sh}+jb_{sh}=1/Z_{sh}$, and g_{sh} and b_{sh} are conductance and susceptance of the shunt bus which STATCOM is connected to, respectively. Fig. 6 depicts the configuration and V - I characteristic of STATCOM

adopted in this paper.

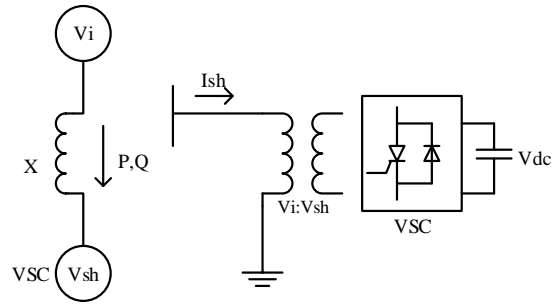


Fig. 4. Fundamental schematic of STATCOM

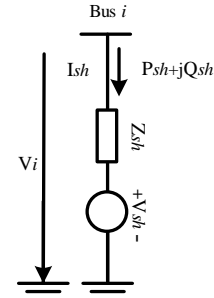


Fig. 5. Equivalent circuit of STATCOM

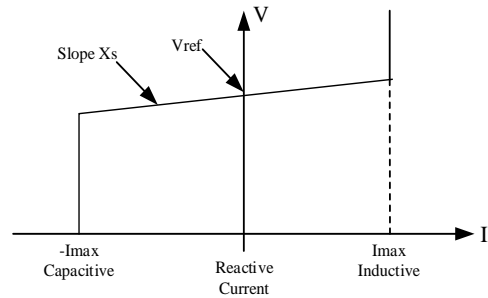


Fig. 6. V-I characteristic of STATCOM

2.3. Unified Power Flow Controller (UPFC)

Unified Power Flow Controller (UPFC) is a compound power electronic device. UPFC concept was introduced in 1991 by L. Gyugyi with the aim of real-time controlling and optimization of power flow in electrical power transmission systems [12]. The configuration of the UPFC is designed by coupling of a shunt and a series voltage source inverter (VSI) via a DC link which comprises a capacitor (C), shown in Fig 7. The basic function of the UPFC is that If the active power flows from series converter into AC system, the DC link voltage will be discharged and if the active power flows from AC system into series converter, the DC link voltage will be charged. So in order to keep the DC link voltage fixed, the shunt converter is used to provide the power demanded by series converter through a common DC link [28]. From the conceptual view point, both active and reactive powers of the line can be controlled by the shunt and series converters of the UPFC smoothly, swiftly, and independently. Implementing UPFC at critical points of the transmission line will increase the

power dispatch up to the power rating of generators and transformers and also expand thermal limits of line conductors, by increasing the stability margins [23].

Based on the equivalent circuit of the UPFC for power flow analysis which is represented in Fig. 8, the phasors V_{sh} and V_{se} represent the equivalent, injected shunt voltage, and series voltage sources, respectively. Z_{sh} and Z_{se} are the UPFC series and shunt coupling transformer impedances, respectively. V_i and V_j are voltages at buses i, j , respectively, while V_k is the voltage of bus k of the receiving-end of the transmission line.

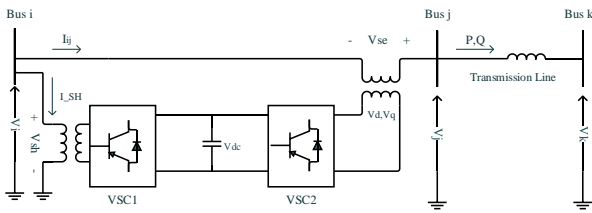


Fig. 7. Fundamental schematic of UPFC

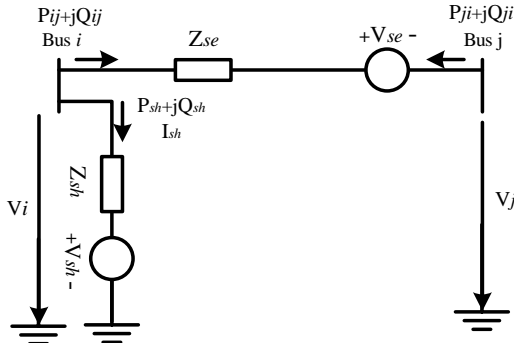


Fig. 8. Equivalent circuit of UPFC

I_{sh} is the current through the UPFC shunt converter. P_{sh} and Q_{sh} are the shunt converter branch active and reactive power flows, respectively. The power flow direction of P_{sh} and Q_{sh} is leaving bus i . I_{ij} and I_{ji} are the currents through the UPFC series converter, and $I_{ij} = -I_{ji}$. P_{ij} and Q_{ij} are the UPFC series active and reactive power flows, respectively, leaving bus i . P_{sh} is the real power exchange of the shunt converter with the DC link. P_{se} is the real power exchange of the series converter with the DC link. Suppose $V_{sh} = V_{sh} \angle \theta_{sh}$, $V_{se} = V_{se} \angle \theta_{se}$, $V_i = V_i \angle \theta_i$, $V_j = V_j \angle \theta_j$; then the power flow of the UPFC shunt and series branches are:

$$P_{sh} = V_i^2 g_{sh} - V_i V_{sh} \left(g_{sh} \cos(\theta_i - \theta_{sh}) + b_{sh} \sin(\theta_i - \theta_{sh}) \right) \quad (5)$$

$$Q_{sh} = -V_i^2 b_{sh} - V_i V_{sh} \left(g_{sh} \sin(\theta_i - \theta_{sh}) - b_{sh} \cos(\theta_i - \theta_{sh}) \right) \quad (6)$$

$$P_{ij} = V_i^2 g_{ij} - V_i V_j \left(g_{ij} \cos \theta_{ij} + b_{ij} \sin \theta_{ij} \right) - V_i V_{se} \left(g_{ij} \cos(\theta_i - \theta_{se}) + b_{ij} \sin(\theta_i - \theta_{se}) \right) \quad (7)$$

$$Q_{ij} = -V_i^2 b_{ij} - V_i V_j \left(g_{ij} \sin \theta_{ij} + b_{ij} \cos \theta_{ij} \right) - V_i V_{se} \left(g_{ij} \sin(\theta_i - \theta_{se}) + b_{ij} \cos(\theta_i - \theta_{se}) \right) \quad (8)$$

The above voltage and power flow control is a very common control method and has been used widely in UPFC models. It has been recognized that besides the power flow control, UPFC has the ability to control angle, voltage and impedance or combination of those in which these abilities will be discussed in details in section IV. Fig. 9 illustrates schematic and V-I characteristic of UPFC.

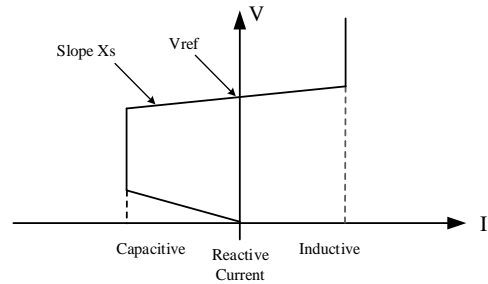


Fig. 9. V-I characteristic of UPFC

3. CASE STUDY

Improving grid fault tolerance is of great importance to avoid cascade failures in the system known as “*Domino effect*”, which may cause major blackouts in the grid. To avoid these failures, all three FACTS devices utilized in this study are supposed to be installed in their best compromised place while having the same rating and operational capacity.

The FRT capability and devices performance in response to different time-domain faults can be deeply compared by consideration of this hypothesis. Fig. 10 shows the system under study. A wind farm consisting of six 1.5 MW wind turbines is connected to a 25-kV distribution system at a point of common coupling (PCC) in order to export power to a 120-kV grid through a 25-km 25-kV feeder, enabling the SCIG-based wind turbines to inject a total of 9MW power into the grid. Unique features of IGs, such as relatively inexpensive price, rigidity, and low maintenance required, with respect to DFIGs, are the reasons to choose IGs in this paper. The stator winding of IG is connected directly to the 60Hz grid, while the rotor is driven by a variable-pitch wind

turbine. The wind turbines are connected via 1km transmission line and Y/Y step up transformer to the ac grid. Under normal operating conditions the reactive power produced by the IG is controlled at zero MVar level to maintain unity power factor. To improve the performance of the IG, aforementioned FACTS devices are connected to the PCC bus to assure the system safe operation.

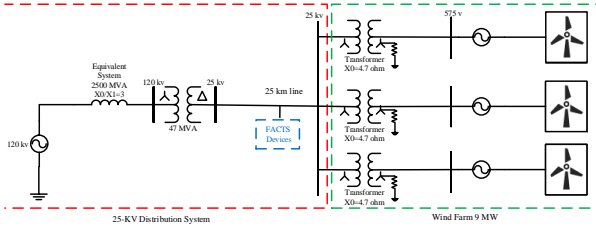


Fig. 10. Schematic diagram of case study

3.1. Wind turbine model

Wind turbine (WT) has blades connected to the mechanical shaft through gearbox and rotor hub. It converts kinetic energy of the wind into mechanical energy of the shaft. The shaft drives the generator to convert the mechanical energy into electrical energy. The energy contained by the wind depends on the wind velocity V and air density ρ . The output mechanical power developed by the WT can be expressed by the following relation [14]:

$$P_{WT} = \frac{1}{2} \rho A v^3 C_p(\lambda, \beta) \quad (9)$$

where A is the area swept by rotor blades; C_p is the power coefficient (or coefficient of performance) of wind turbine which is a non-linear function of tip-speed ratio λ and the blade pitch angle β and obviously different for each wind turbine. The power coefficient C_p is defined as follow:

$$C_p(\lambda, \beta) = \frac{1}{2} \left(\frac{98}{\lambda_i} - 0.4\beta - 5 \right) \exp\left(\frac{-16.5}{\lambda_i}\right) \quad (10)$$

3.2. Induction generator model

The typical model for the induction generator is adopted in this paper [24]. The Dynamic or d-q equivalent circuit of an induction machine is shown in Fig. 11. The modeling equations of a squirrel cage induction machine in state-space can be deduced [25].

$$\frac{d\varphi_{qs}}{dt} = \omega_b \left[v_{qs} - \frac{\omega_e}{\omega_b} \varphi_{ds} + \frac{R_s}{x_{ls}} \left(\frac{x_{ml}^*}{x_{lr}} \varphi_{qr} + \left(\frac{x_{ml}^*}{x_{ls}} - 1 \right) \varphi_{qs} \right) \right] \quad (11)$$

$$\frac{d\varphi_{ds}}{dt} = \omega_b \left[v_{ds} - \frac{\omega_e}{\omega_b} \varphi_{qs} + \frac{R_s}{x_{ls}} \left(\frac{x_{ml}^*}{x_{lr}} \varphi_{dr} + \left(\frac{x_{ml}^*}{x_{ls}} - 1 \right) \varphi_{ds} \right) \right] \quad (12)$$

$$\frac{d\varphi_{qr}}{dt} = \omega_b \left[-\frac{(\omega_e - \omega_b)}{\omega_b} \varphi_{dr} + \frac{R_r}{x_{ls}} \left(\frac{x_{ml}^*}{x_{lr}} \varphi_{qs} + \left(\frac{x_{ml}^*}{x_{ls}} - 1 \right) \varphi_{qr} \right) \right] \quad (13)$$

$$\frac{d\varphi_{dr}}{dt} = \omega_b \left[\frac{(\omega_e - \omega_b)}{\omega_b} \varphi_{qr} + \frac{R_r}{x_{ls}} \left(\frac{x_{ml}^*}{x_{lr}} \varphi_{ds} + \left(\frac{x_{ml}^*}{x_{ls}} - 1 \right) \varphi_{dr} \right) \right] \quad (14)$$

$$\frac{d\omega_r}{dt} = \left(\frac{p}{2J} \right) (T_e - T_L) \quad (15)$$

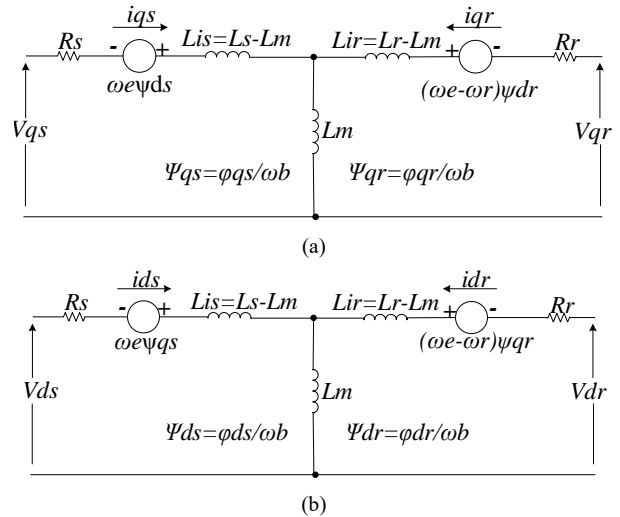


Fig. 11. Dynamic or d-q equivalent circuit of an induction machine

4. COMPARISON OF FACTS IN POINT OF CONTROL THEORY

The aim of this section is to present an argumentative mathematical scenario and control analysis of three FACTS devices studied in this paper in order to provide readers a tangible view. The control systems of SSSC, STATCOM, and UPFC devices are provided in Figs 12, 13, and 14, respectively. As one can be seen in these control systems, SSSC utilizes connected buses voltages, V_i and V_j , capacitor DC voltage, VDC, and line current, I_{ij} , to finally produce the switching pulses necessary for its voltage-source converter (VSC). However, STATCOM is using voltage of the bus which it is

connected to in shunt (V_i), line converter (VSC). However, STATCOM is using voltage of the bus which it is connected to in shunt (V_i), line current, I_{ij} , and DC voltage, VDC to produce these essential pulses required for the VSC to act. It uses a dual voltage regulation loop, an inner current control loop, and an outer loop regulating AC and DC voltages, which separately achieve in phase and in quadrature reference currents, I_{dref} and I_{qref} . Though, both SSSC and STATCOM utilize the DC voltage of their capacitor and regulate this voltage to obtain in phase converter voltage, V_{d-Conv} , and in phase reference current, I_{dref} , necessary for pulse-width modulation (PWM) technique and producing pulses for converters switching. To this end, both SSSC and STATCOM converter switching is dependent on the DC link voltage. In simple words, charging and discharging of the capacitor as a fixed DC voltage source is making troubles for SSSC and STATCOM converters switching under some circumstances, while implementing a fixed DC voltage source can amend this drawback straightforwardly.

As shown in Fig. 14, control of UPFC is carried out by utilizing bus voltages in which UPFC is connected to, V_i and V_j , and line current, I_{ij} . The in phase and quadrature voltages and currents are measured to calculate active and reactive power, P and Q. In phase and quadrature voltages, V_d and V_q , are then provided to the PWM modulator in order to produce PWM pulses. Despite SSSC, which two degrees of freedom of the series converter are used to control the DC voltage and the reactive power, in case of a UPFC three degrees of freedom are used to control the line active and reactive power, as well as an additional degree of freedom which is shunt converter voltage, V_i . Shunt converter controls its voltage by absorbing or generating reactive power. Table 1 provide a more tangible view about the main control rules and parameters and relating distinctive features of all FACTS devices used in these paper in point of controllability.

Controllability of UPFC can be better understood by phasor diagram of its currents and voltages as depicted in Fig 15. UPFC topology provides much more flexibility for controlling the line active and reactive power because active power can be transferred from the shunt converter to the series converter, through the DC link. Contrary to the SSSC where the injected voltage V_{se} is constrained to stay in quadrature with line current I_{ij} , the injected voltage V_{se} can now have any angle with respect to line current. If the magnitude of injected voltage V_{se} is kept constant and if its phase angle ϕ with respect to V_i is varied from 0 to 360 degrees, the locus described by the

end of vector V_j ($V_j=V_i+V_{se}$) is a circle as shown on the phasor diagram.

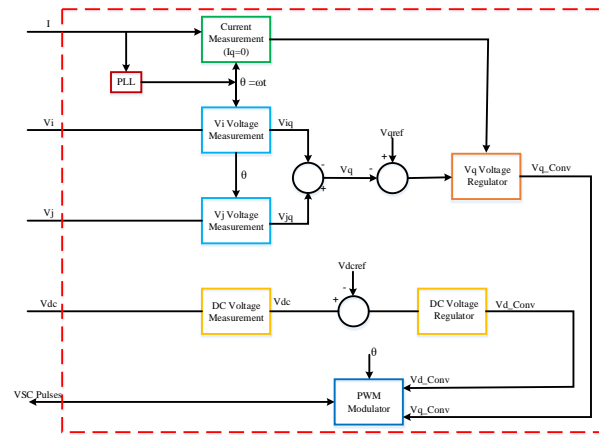


Fig. 12. SSSC Control System

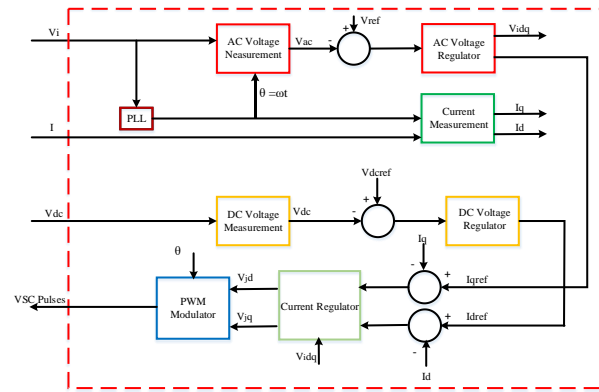


Fig. 13. STATCOM Control System

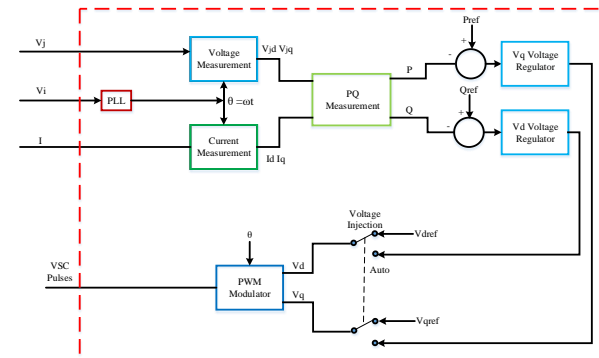


Fig. 14. UPFC Control System

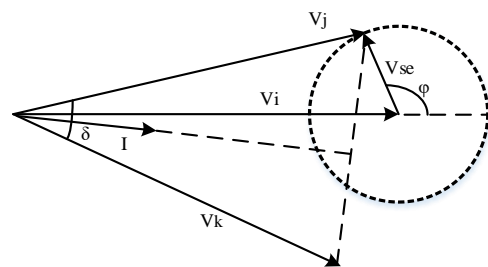


Fig. 15. UPFC Current and Voltages Phasor Diagram

As ϕ is varying, the phase shift δ , angle between two voltages vectors V_j and V_k , also varies. It follows that both

the active power P and the reactive power Q transmitted at one-line end can be controlled. Therefore, when a fault occurs in the wind farm connecting to a power system, it is vital for the operators to provide or withdraw enough reactive and active power if the secure operation of the system is desired. The effectiveness of a FACTS device is dramatically dependent on configuration of the system and reactance beyond the bus at which the device is connected. The impact of system fault level on feasible operating area of a FACTS device can be determined by analysing device influence on effective reactance of the transmission line.

Table 1. Control Theory Perspective of SSSC, STATCOM, and UPFC.

FACTS	Control Inputs	Main Control Rules	Distinctive Features
SSSC	I, V_i, V_j, V_{dc}	DC Voltage Measurement	2 degree of freedom, Capacitor charging and discharging
STATCOM	I, V_i, V_{dc}	DC Voltage Measurement	2 degree of freedom, Capacitor charging and discharging
UPFC	I, V_i, V_j	PQ Measurement	3 degree of freedom, Independency of DC regulation

5. SIMULATION RESULTS

When a fault occurs in the wind farm connecting to a power system, it is vital for the operators to provide or withdraw enough reactive and active power if the secure operation of the system is desired. The effectiveness of a FACTS device is dramatically dependent on configuration of the system and reactance beyond the bus at which the device is connected. The impact of system fault level on feasible operating area of a FACTS device can be determined by analyzing device influence on effective reactance of the transmission line.

In this section, by installing SSSC, STATCOM and UPFC devices in the system under study in order to appreciate the behavior of the system during the occurrence of fault, simulations are carried out for two different time-domains of short-term and long-term faults and their performances are investigated. The case Without FACTS devices is also considered in order to provide a comparable study. The performance of these devices is scrutinized in two main cases. In case one, performance of these devices in relation to voltage sag of PCC bus at the time fault experienced in the system is studied. In the second case, they are compared in point of their dynamic responses and also percentage of their compensation. To investigate the impact of the proposed FACTS devices in this paper a three phase-to-ground

short circuit fault is applied to the system at the PPC bus at time $t=5s$. Fault clearance duration for the short-term fault is considered 50ms and for long-term fault this time is assumed 110ms. The compensation capability of all these three devices is adopted equal to 3MVA. It is notable that in order to evaluate and compare the influence of SSSC, STATCOM, and UPFC on the system stability margins, repeated simulations were carried out to determine the most reasonable response. Parameters of a single 1.5-MW IG in network system is presented in Table 3. Table 4 displays the parameters of converters in all FACTS devices.

5.1. Voltage sag events

In pre-fault situation, the voltage of PPC bus for STATCOM and UPFC cases is 0.9749 pu, while for the case with SSSC or without FACTS devices the voltage is 0.8949 pu. This small difference between the voltages in pre-fault situation between shunt and series devices is due to the shunt part of STATCOM and UPFC in this way that they affect line voltage by direct injecting or withdrawing reactive power to the line while series devices like SSSC only affect transmission line reactance and in this way improve transient stability. In case of short-term fault, when fault is initiated considerable voltage sags of the nominal value are experienced by the system under study. As it is shown for short-term fault in Fig. 16, during the voltage sag event SSSC could not tolerate the fault and after clearance of fault it did not help the system and continued like the case without using FACTS devices. However, in case of UPFC and STATCOM, they moderately experienced the same speed overshooting and settling time and voltage profile achieved higher values in steady-state.

Table 2. Voltage sag fluctuations of SSSC, STATCOM and UPFC in per-unit

FACTS Devices	Pre-fault	Post-fault	
		Short-term	Long-term
Without FACTS	0.8949	0.6328	0.6328
SSSC	0.8949	0.6328	0.6328
STATCOM	0.9749	0.9749	0.6706
UPFC	0.9749	0.9749	0.9749

When long-term fault is initiated to the system, all three devices reasonably experienced the same voltage sags as for short-term due to the fact that all devices are affected by short-circuit fault applied to PCC bus, but after clearance of fault SSSC and STATCOM were incapable of keeping up the bus voltage while UPFC brilliantly restored the PCC voltage and the electrical torque of IG in fault situation. Fig 17 illustrates the voltage sag during long-term fault. The obtained results for voltage sag of these three devices for both short-term and long-term domains can be found in Table 2.

Table 3. Parameters of a Single 1.5-MW IG in Network System.

Nominal Wind Turbine Output Power	1.5 MW
Rated Voltage	575v
Frequency	60 Hz
$R_s(\Omega)$	0.006863 pu
$XL_s(\Omega)$	0.1286 pu
$R_r(\Omega)$	0.006377 pu
$XL_r(\Omega)$	0.1791 pu
$X_M(\Omega)$	6.77 pu

Table 4. Parameters of Converters in all FACTS Devices.

Nominal Voltage (V_{rms})	25 kv
Frequency	60 Hz
Converter Rating	3 MVA
DC line Nominal voltage	4 kv

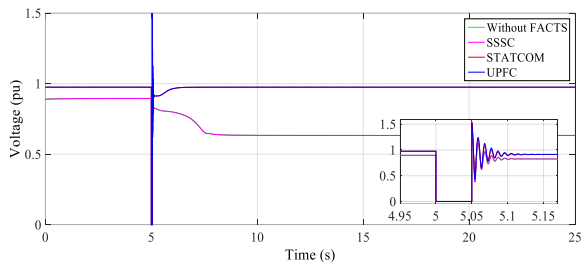


Fig. 16. Voltage sag of SSSC, STATCOM, UPFC, and Without FACTS for short-term faults.

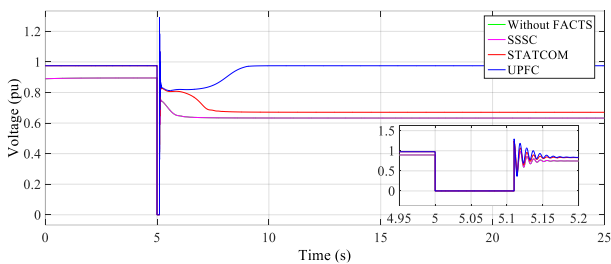


Fig. 17. Voltage sag of SSSC, STATCOM, UPFC, and Without FACTS for long-term faults.

5.2. Dynamic response

Figs. 18 and 19 show the short-term and Figs. 20 and 21 illustrate the long-term active and reactive power exchanges between the IG and the grid, respectively. As it can be perceived, during the short-term faults STATCOM and UPFC show somewhat the same responses, while SSSC cannot improve the active power after fault clearance and system responded as if the system operates without FACTS devices; however, when the system is exposed to faults SSSC and STATCOM proved inability to maintain the safety margins of the system however, UPFC magnificently prevents active power and held on to 8.93MW within less than 4 seconds. Therefore, after the clearance of fault, the active power is restored to its pre-fault level. Moreover, SSSC and STATCOM absorb large amount of reactive power, about 12.2Mvar, from the grid in short-term fault situation in comparison with UPFC, which is 5Mvar. In long-term fault situation, SSSC and STATCOM absorb even more of that amount. STATCOM absorbed around

13Mvar, 1Mvar more than SSSC due to aforementioned reasons, which is quite a burden into the system under such severe conditions. However, by utilization of UPFC, the absorbing reactive power from the grid is significantly reduced, almost the same as for short-term which was 5Mvar, that helps to avoid other problems, such as voltage collapse.

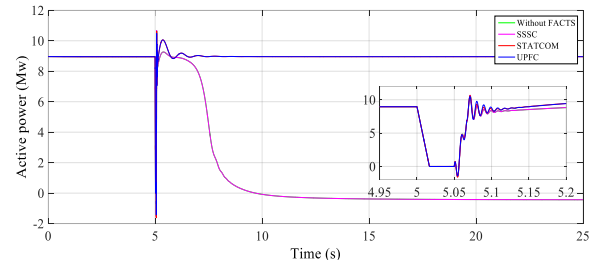


Fig. 18. Active power responses of SSSC, STATCOM, UPFC, and Without FACTS for short-term faults.

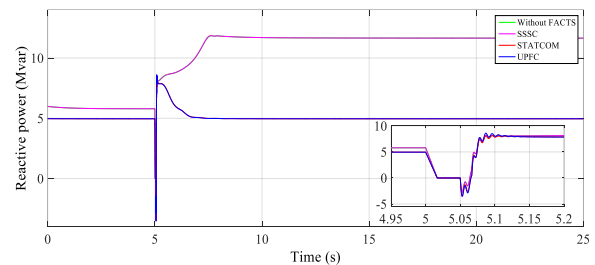


Fig. 19. Reactive power responses of SSSC, STATCOM, UPFC, and Without FACTS for short-term faults.

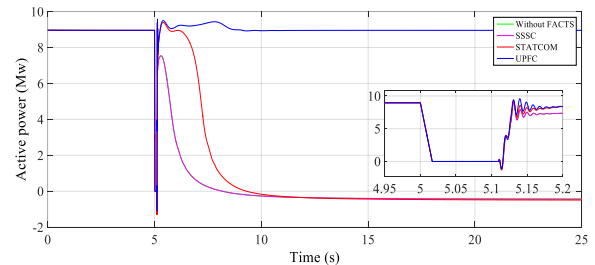


Fig. 20. Active power responses of SSSC, STATCOM, UPFC, and Without FACTS for long-term faults.

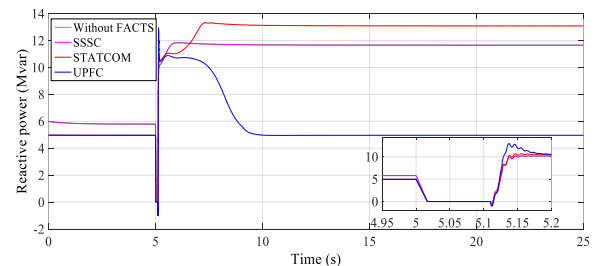


Fig. 21. Reactive power responses of SSSC, STATCOM, UPFC, and Without FACTS for long-term faults.

6. CONCLUSION

In this paper, the performances of SSSC, STATCOM, and UPFC FACTS devices with the same rating and operational capacity encountered with short-term and long-term time-domain faults are studied. For short-term faults, SSSC despite STATCOM and UPFC is

unsuccessful in maintaining system voltage profile by falling to 0.63 pu and active power to zero. STATCOM shows promising results under short-term faults by keeping its voltage profile to 0.97 pu, but it fails to encounter with long-term faults with the same trend for SSSC. The improvement of the voltage profile after the clearance of long-term faults is obvious in UPFC case, in comparison with SSSC and STATCOM. UPFC is capable of improving voltage 30% and 34% more than STATCOM and SSSC devices, respectively. Regarding to active and reactive power compensation, both SSSC and STATCOM are unable to maintain system stability when system is exposed to long-term faults. In these cases, their real and reactive power dramatically decrease to cause instability of the system; however, UPFC successfully maintained system active power by keeping it up to 9MW with only 5Mvar reactive power compensation required after fault clearance. Simulation results authenticate that UPFC significantly aids wind energy conversion system (WECS) to keep up its voltage and power requirement at the desired rate and guarantees system protection. This capability owes to the shunt and series parts of UPFC and their collaboration besides the independent feature of UPFC in regulating DC voltage. As a result, UPFC can be suggested for systems that need to be tolerant against faults and require high protection levels.

REFERENCES

- [1] S. M. Z-Hosseini; M. O. Buygi. "How Does Large-scale Wind Power Generation Affect Energy and Reserve Prices?," *J. Oper. Autom. Power Eng.*, vol. 6, no. 2, pp. 169-182, 2018.
- [2] K. V. Dave, S. M. Kanani. "Use of SVS for stability improvement analysis in wind farm by SVC during fault," *Int. J. Eng. Sci. Res.*, vol. 6, no. 1, pp. 43-48, 2016
- [3] M. Moradzadeh, H. Shayeghi, L. Vandeveld and M. Saif, "Impact of increased penetration of large-scale wind farms on power system dynamic stability-A review," *Proce. IEEE 15th Int. Conf. Environ. Electr. Eng.*, Rome, pp. 1522-1526, 2015.
- [4] J. M. Rodriguez and J. L. Fernandez, "Incidence on power system dynamics of high penetration of fixed speed and doubly fed wind energy systems: study of the Spanish case" *IEEE Trans. Power Syst.*, vol. 17, no. 4, 2002.
- [5] H. S. Ko, G. G. Yoon, and W. P. Hong, "Active use DFIG-based variable- speed wind-turbine for voltage control in power system operation" *J. Elect. Eng. Technol.*, vol. 3, no. 2, pp. 254-262, 2008.
- [6] R. Grunbaum, "FACTS for grid integration of wind power" *Proce. IEEE PES Innovative Smart Grid Technol. Conf. Eur.*, 2010, pp. 1-8.
- [7] M. T. Hagh, "Dynamic and stability improvement of a wind farm connected to grid using UPFC," *Proce. IEEE Int. Conf. Ind. Technol.*, 2008, pp. 1-5.
- [8] M. Ferdosian, H. Abdi and A. Bazaei, "Improved dynamic performance of wind energy conversion system by UPFC," *Proce. IEEE Int. Conf. Ind. Technol.*, Cape Town, 2013, pp. 545-550.
- [9] Ghasemi and C. A. Canizares, "Validation of a STATCOM transient stability model through small-disturbance stability studies," *Proce. IEEE Int. Conf. Syst. Eng.*, San Antonio, TX, 2007, pp. 1-6.
- [10] Y. M. Alharbi and A. Abu-Siada, "Application of UPFC to improve the low-voltage-ride-through capability of DFIG," *Proce. IEEE 24th Int. Symp. Ind. Electron.*, Buzios, 2015, pp. 665-668.
- [11] L. Gyugyi, "Unified power-flow control concept for flexible AC transmission systems," *Proc. Inst. Elect. Eng. C*, vol. 139, no. 4, pp. 323-331, 1992.
- [12] J. Dixon, L. Moran, J. Rodriguez and R. Domke, "Reactive power compensation technologies: state-of-the-art review," *Proce. IEEE*, vol. 93, no. 12, pp. 2144-2164, 2005.
- [13] C. C. A. Rajan, A. Chodisetty, K. M. Raju and T. Srikumar, "Design and simulation of STATCOM to enhance the voltage stability of a wind power system," 2015 International Conference on Electrical, Electronics, Signals, *Commun. Optimiz.*, Visakhapatnam, 2015, pp. 1-4.
- [14] S. Gautam, C. Pang and L. Yang, "Impacts of FACTS device on wind farm protection: Comparison between STATCOM and UPFC," *Proce. 7th Int. Conf. Inf. Autom. Sustain.*, Colombo, 2014, pp. 1-6.
- [15] S. N. Singh and A. K. David, "Placement of FACTS devices in open power market," *Proce. Int. Conf. Adv. Power Syst. Control Oper. Manag.*, 2000, pp. 173-177 vol.1.
- [16] N. Hingorani and L. Gyugyi, *Understanding FACTS: Concepts and Technology of Flexible AC Transmission Systems*. New York, NY, USA: *Wiley IEEE*, 1999.
- [17] Dinh-Nhon Truong, Van-Thuyen Ngo, "Designed damping controller for SSSC to improve stability of a hybrid offshore wind farms considering time delay," *Int. J. Electr. Power Energy Syst.*, vol. 65, pp. 425-431, 2015.
- [18] S. Raphael, A. M. Massoud, "Static synchronous series compensator for low voltage ride through capability of wind energy systems," *Proce. Int. Conf. IET Renew. Power Gener.*, Edinburgh (UK), pp. 1-6, 2011.
- [19] S. M. Abd Elazim, E. S. Ali, "Optimal SSSC design for damping power systems oscillations via Gravitational Search Algorithm", *Electr. Power Energy Syst.*, pp. 161-168, 2016.
- [20] K. K. Sen, "SSSC-static synchronous series compensator: theory, modeling, and application," *IEEE Trans. Power Delivery*, vol. 13, no. 1, pp. 241-246, 1998.
- [21] N. Mohan, T. Undeland, and W. Robbins, "Power Electronics: Converters, Applications, and Design". New York: *Wiley*, 2003.
- [22] H. Akagi, E. H. Watanabe, M. Aredes. "Instantaneous power theory and applications to power conditioning" in *IEEE Ind. Electron. Mag.*, vol. 1, no. 3, pp. 46-46, 2007.
- [23] M. E. Adabi, A. Vahedi, "A survey of shaft voltage reduction strategies for induction generators in wind energy applications," *Renew. Energy*, vol. 50, pp. 177-187, 2013.
- [24] B. Ozpineci and L. M. Tolbert, "Simulink implementation of induction machine model-a modular approach," *Proce. Int. IEEE Conf. Electr. Mach. Drives*, vol.2, pp. 728-734, 2003.
- [25] MEA. Farrag, GA. Putrus, L Ran, "Design of fuzzy based-rules control system for the unified power flow controller," *Proce. IEEE*, Piscataway, NJ, pp. 2102-2107.

- [26] M. S. El Moursi, K. Goweily, J. L. Kirtley and M. Abdel-Rahman, "Application of series voltage boosting schemes for enhanced fault ride through performance of fixed speed wind turbines," *IEEE Trans. Power Delivery*, vol. 29, no. 1, pp. 61-71, 2014
- [27] M. Nasiri; J. Milimonfared; S. H. Fathi. "Efficient low-voltage ride-through nonlinear backstepping control strategy for PMSG-based wind turbine during the grid faults," *J. Oper. Autom. Power Eng.*, vol. 6, no. 2, pp. 218-228, 2018.
- [28] N. Bigdeli; E. Ghanbaryan; K. Afshar. "Low frequency oscillations suppression via cpso based damping controller," *J. Oper. Autom. Power Eng.*, vol. 1, no. 1, pp. 22-32, 2007.